# Profile-turbulence interactions, magnetohydrodynamic relaxations, and transport in tokamaks

A. Thyagaraja, P. J. Knight, M. R. de Baar, G. M. D. Hogeweij, and E. Min

Citation: Physics of Plasmas **12**, 090907 (2005); doi: 10.1063/1.2034387
View online: http://dx.doi.org/10.1063/1.2034387
View Table of Contents: http://scitation.aip.org/content/aip/journal/pop/12/9?ver=pdfcov
Published by the AIP Publishing



# Profile-turbulence interactions, magnetohydrodynamic relaxations, and transport in tokamaks

A. Thyagaraja and P. J. Knight
*European Atomic Energy Community (EURATOM)/United Kingdom Atomic Energy Authority (UKAEA) Fusion Association, Culham Science Centre, Abingdon, OX14 3DB, United Kingdom*

M. R. de Baar, G. M. D. Hogeweij, and E. Min
*Association of European Atomic Energy Community (EURATOM)-Fundamental Ondorzoek der Materie (FOM), Trilateral Euregio Cluster, P.O. Box 1207, 3430 BE Nieuwegein, The Netherlands*

(Received 16 March 2005; accepted 2 May 2005; published online 21 September 2005)

The dynamical behavior of the global, two-fluid, electromagnetic model of a tokamak plasma is explored under conditions corresponding to the Rijnhuizen tokamak project [A. J. H. Donné, Plasma Phys. Rep. **20**, 192 (1994)] using the CUTIE code [A. Thyagaraja, Plasma Phys. Controlled Fusion **42**, B255 (2000)]. Simulations of an off-axis electron-cyclotron-heated (350 kW) hydrogen discharge and a purely Ohmic one over several resistive evolution times ($\tau_{\mathrm{res}} \simeq 15-20$ ms) are described. The results illustrate profile-turbulence interactions and the spectral transfer processes implicated in the spontaneous generation and maintenance of mesoscale zonal flows and dynamo currents. Relaxation phenomena, including off- and on-axis sawteeth and periodically repeating edge ballooning instabilities mediated by these mechanisms, are presented. The CUTIE model reproduces many observed features of the experiment qualitatively and suggests that global electromagnetic simulations may play an essential role in understanding tokamak turbulence and transport. [DOI: 10.1063/1.2034387]

## I. INTRODUCTION

Tokamak plasmas of interest in fusion research have many remarkable features associated with the complex interactions between profiles of density, current, temperature, and flows and electromagnetic turbulence. The key ingredients of the evolutionary dynamics of strongly driven dissipative systems (such as tokamaks or the ocean-atmosphere climatalogical geosystem) can be identified: existence of large reservoirs/sources of free-energy, a huge range in scales of motion simultaneously present, strong nonlinearities which make predictions based on linear theory questionable, significant profile-turbulence interactions via nonlinear mechanisms local in position space but strongly nonlocal in wave number and frequency, and tendency of the system to "self-organize" spatially and temporally. In tokamaks, typical sources of instability are in the gradients of density, pressure, current, and flow. Tokamaks also exhibit phenomena such as internal transport barriers (ITBs), or regions of significantly reduced local radial transport and turbulence in common with geophysical systems. ITBs in tokamak plasmas involve "zonal flows" and the safety factor/current profiles, while in geophysics, a closely related "shear-sheltering" phenomenon is implicated[1] in transport reduction. Both systems exhibit spectral transfer processes involving both "direct" (phase mixing, vortex/current stretching) and "inverse" (modulational instability) cascades, as elucidated originally by Hasegawa and Kodama[2] and more recently by many others using more detailed models.[3–5]

We have investigated, in a number of publications,[6–8] the two-fluid, quasineutral, electromagnetic plasma model as a tool for understanding some of these features. In this paper, we present examples drawn from extensive computations using the CUTIE code based on this model. The plan of the paper is as follows. In Sec. II we briefly review the key assumptions of the model and the specifics of the code pertaining to the examples presented. Sec. III considers the results obtained using CUTIE in two specific experimentally relevant situations. We present some conclusions in Sec. IV.

## II. THE TWO-FLUID MODEL: CUTIE

We very briefly review the key ideas of the quasineutral two-fluid model, as embodied in the CUTIE code. Extensive details are available elsewhere.[6–8] This model provides a "minimal" extension to the well-known viscoresistive magnetohydrodynamics (MHD) model. The plasma consists of electrons and a single species of ions, which may be assumed to be hydrogen or deuterium; we take $n_e \simeq n_i = n$ and $\mathbf{j} = c/4\pi \nabla \times \mathbf{B}$ ("quasineutrality"). Each species is assumed to be locally Maxwellian, but $T_i$ is not necessarily equal to $T_e$. The model does not account for kinetic/velocity space (linear or nonlinear) effects. On the other hand, many drift effects[10] ignored by MHD are included, as well as a "generalized Ohm's law." A large aspect ratio $R/a \gg 1$ tokamak ordering, $B_{\mathrm{pol}} \ll B_{\mathrm{tor}}, \beta \ll 1, k_{\|} \ll k_{\perp}$, is used in the model which includes field-line bending and curvature but neglects some stabilizing effects (due to Shafranov shifts). Neoclassical theory[10] is assumed to provide a minimum level of transport. Particle and energy source profiles (except Ohmic heating) are not calculated in detail, but simply prescribed in accordance with transport codes. Conservation equations for particles, energy, and momentum and Maxwell's equations are solved (see Refs. 7 and 8) to obtain $T_{e,i}, n$, ion velocity $\mathbf{v}$, electrostatic potential $\Phi$, and parallel vector potential $\Psi$. Mesoscales, time scales between the Alfvén time [$\tau_{\mathrm{A}} = qR_0/V_A$,

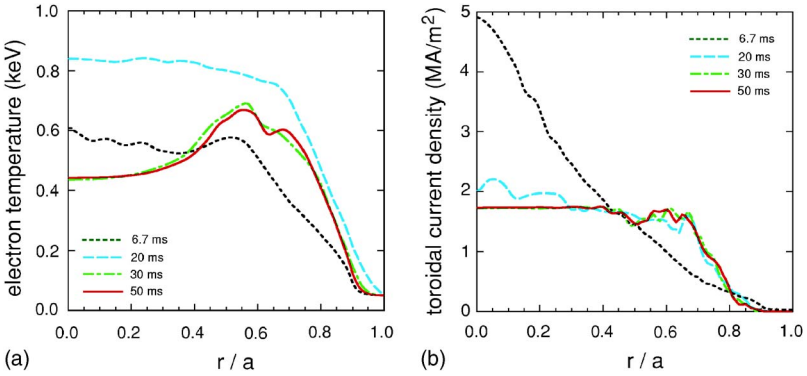


FIG. 1. Evolution of the (a) $T_e$ and (b) $j_{\mathrm{tor}}$. RTP off-axis ECH (350 kW).

$V_A = B_{\mathrm{tor}}/(4\pi m_i n_e)^{1/2}$] and the resistive time ($\tau_{\mathrm{res}} = 4\pi a^2/c^2\eta_{\mathrm{nc}}$), and length scales $L_{\mathrm{meso}}$ satisfying $\rho_s < L_{\mathrm{meso}} < a$ are modeled, where $\Omega_{ci} = eB_{\mathrm{tor}}/m_i c$ and $\Omega_{ci}^2\rho_s^2 = C_s^2 = (T_i + T_e)/m_i$. A key feature of CUTIE is the coevolution of flux-surface-averaged quantities and the turbulence on the turbulence time scale (resolving shear Alfvénic modes). In summary, CUTIE contains the following fluid-like modes: linear and nonlinear shear Alfvén waves, slow magneto acoustic modes, drift-tearing modes, and ballooning (ideal and viscoresistive branches) modes; the fluid branch of the ion-temperature-gradient (ITG)-driven instability is also included. It should be noted that purely viscoresistive MHD equations do not allow for the following key two-fluid effects simulated by CUTIE: transport fluxes, real-frequency spectra of turbulent fluctuations, drift-wave ($\omega_*$ effects) modifications on the mesoscale, zonal flow effects, and ITG-driven instabilities. In CUTIE trapped particle kinetic effects[9] on turbulent dynamics are neglected (as are electron temperature gradient modes). When subject to external sources, the system gives rise to turbulence with regions of mesoscale variations of profiles called "corrugations." These profile gradients interact ("cross-talk") nonlinearly with the turbulence. The poloidal magnetic field (consequently the safety factor, $q = rB_{\mathrm{tor}}/RB_\theta$) evolves in time and space according to the induction equation:

$$\frac{\partial\langle B_\theta\rangle}{\partial t} = c\frac{\partial\langle E_\zeta\rangle}{\partial r}, \tag{1}$$

where $\langle\cdots\rangle$ denotes averaging over a flux surface, and $\langle E_\zeta\rangle = \eta_{\mathrm{nc}}(\langle j_\zeta\rangle - j_{\mathrm{bs}} - j_{\mathrm{dyn}})$. The "dynamo current," $j_{\mathrm{dyn}} = \langle\hat{\mathbf{e}}_\zeta.(\delta\mathbf{v}\times\delta\mathbf{B})\rangle/c\,\eta_{\mathrm{nc}}$ is driven by the correlations between turbulent fluctuations of $\mathbf{v},\mathbf{B}$. In the foregoing equation, we use standard neoclassical expressions for the resistivity $\eta_{\mathrm{nc}}$ and the bootstrap current $j_{\mathrm{bs}}$,[10] respectively. The total toroidal current is related to the poloidal field as usual through Ampère's law: $j_\zeta \equiv j_{\mathrm{tor}} = c/4\pi 1/r\partial rB_\theta/\partial r$. The radial electric field, $\langle E_r\rangle$, is determined by averaging the radial momentum balance relation,

$$E_r = \hat{\mathbf{e}}_r\cdot\left(-\frac{\mathbf{v}\times\mathbf{B}}{c} + \frac{1}{en}\nabla p_i\right). \tag{2}$$

The poloidal flow velocity (toroidal flows are included in CUTIE but are not significant in the examples considered) satisfies

$$\frac{\partial\langle u_\theta\rangle}{\partial t} = -\nu_{\mathrm{nc}}[\langle u_\theta\rangle - u_{\mathrm{nc}}] + \langle L_\theta\rangle, \tag{3}$$

where $\nu_{\mathrm{nc}}$ is the flow-damping rate and $u_{\mathrm{nc}}$ is the poloidal velocity in neoclassical theory.[10] The poloidal acceleration due to turbulence is given by $\langle L_\theta\rangle = -1/r\partial/\partial r(r\langle\delta u_\theta\delta u_r\rangle) + \hat{\mathbf{e}}_\theta.\langle\delta\mathbf{j}\times\delta\mathbf{B}\rangle/m_i n$. These equations and the particle and energy transport equations of a similar structure,[7,8] determine the self-consistent evolution of relevant profiles. The structure of turbulent fluxes shows that rapid local variation of the turbulent fluctuations causes rapid local evolution of the zonal flows and dynamo currents crucial to self-organization. CUTIE is a "large eddy simulation" (LES) code which needs some mechanism to prevent energy transmitted to subgrid scales from spuriously reappearing at long wavelengths ("aliasing"). Indeed, shear Alfvén waves and flows provide an extremely efficient mechanism to transfer energy (and more particularly enstrophy) by a "direct cascade" to sub-ion-gyroradius scales, where kinetic effects randomize

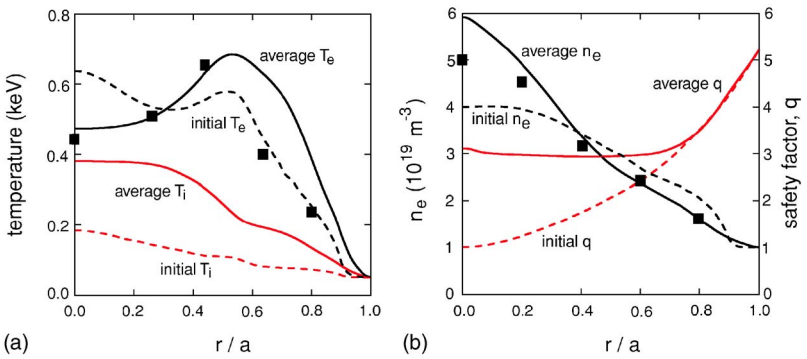


FIG. 2. Theory (solid line) and experiment (squares) comparison of time-averaged (a) $T_e$ and (b) $n_e$.

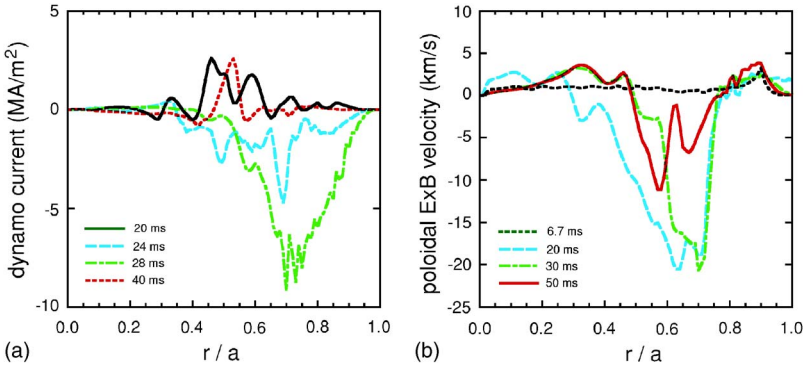


FIG. 3. (a) Dynamo currents and (b) zonal flows. RTP off-axis ECH (350 kW).

phases and prevent energy from returning coherently to longer wavelengths. The net effect of such "phase-mixing"[7] is turbulent diffusion in both real and spectral space. On the other hand, the strongly advective character of the fluxes at the longer, modeled wavelengths is retained explicitly. The objective of CUTIE is to explore the qualitative predictions of the two-fluid model over time scales far longer than the typical turbulent decorrelation times, namely, on at least the resistive time scales. Thus quantitative accuracy is not expected in view of the approximations of the model.

## III. CUTIE SIMULATIONS

The CUTIE model is well suited for exploring long-term evolution studies in small tokamaks which tend to have $\rho_* = \rho_s/a \simeq 10^{-2}$ and reasonably short resistive times ($\simeq 15-20$ ms). For these reasons, we present simulations pertaining to the Rünhuizen tokamak project (RTP) tokamak[11–13] which was a small, well-diagnosed experiment (major radius $R=0.72$ m, minor radius $a=0.16$ m, aspect ratio $R_0/a=4.4$), with dominant electron cyclotron heating (ECH). Our first example is concerned with an off-axis ECH (350 kW) hydrogen discharge. The conditions are plasma current $I_p=80$ kA, toroidal field $B_{\mathrm{tor}}=2.24$ T, and line-average density $\bar{n}_e \simeq 3\times 10^{19}$ m$^{-3}$. These correspond to $\beta = 4\pi\bar{p}/B_{\mathrm{tor}}^2 \simeq 0.2\%$, $\rho_* = \rho_s/a \simeq 0.01$, and $\nu_* = (a/R_0)^{-3/2}[q_a R_0/(V_{\mathrm{the}}\bar{\tau}_e)] \simeq 1$, where $\bar{p}$ is the volume-averaged total pressure, $V_{\mathrm{the}}^2 = 2\bar{T}_e/m_e$, $\bar{T}_e$ is the averaged electron temperature, and $\bar{\tau}_e$ is the averaged electron Braginskii collision time. The ECH power is deposited at $r_{\mathrm{dep}}/a = 0.55$ with a localization of approximately 1 cm. This simulation has been presented in an earlier paper,[8] showing that CUTIE was able to qualitatively account for the off-axis maximum in the electron temperature profile, the global confinement time (3–4 ms), as well as the "sawtooth-like" relaxation oscillations observed in the experiment. Here we present some further details illustrating the role of profile evolution and reorganization due to "corrugated" zonal flows and dynamo currents. We illustrate the computed evolution, starting from an arbitrary initial state at 6 ms up to a final epoch of 50 ms, of the $T_e$ [Fig. 1(a)] and $j_{\mathrm{tor}}$ [Fig. 1(b)] profiles. During the first 20 ms the turbulence and the profiles coevolve to reach a statistically stationary state. After this period we obtain regular relaxation oscillations superposed on a temperature profile with an off-axis maximum and a self-consistent broad current profile. It is a remarkable experimental observation[8] that the $T_e$ profile is inverted despite the fact that the electron-ion equilibration and radiation in the experiment do not provide a strong enough sink of energy. CUTIE is able to reproduce this feature [Fig. 2(a)] as a consequence of a strong outward advective flux in the core.[8] We have plotted some experimental points from Thomson measurements (single time) of $T_e$ and $n_e$. Here and elsewhere, to aid clarity, only a few of the experimental points across the minor radius are plotted. The actual spatial resolution of the Thomson measurements is about 1 cm. CUTIE is in fair agreement inboard of the heating radius with measured temperatures. It predicts somewhat higher confinement outside the heating radius than is observed; this could possibly be due to the neglect of trapped electron mode transport in the model. The density peaking [Fig. 2(b)] in the experiment is somewhat less than CUTIE predictions, possibly due to the centrally peaked particle source (experimental source distribution was not known) used in the simulations.[8] The corresponding $q$ profile (N.B. $T_i$ and $q$ were not measured in

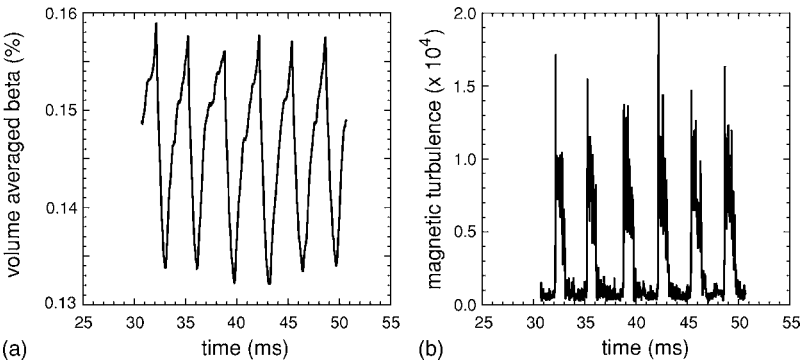


FIG. 4. (a) Volume-averaged $\beta$ and (b) magnetic turbulence. RTP off-axis ECH (350 kW).

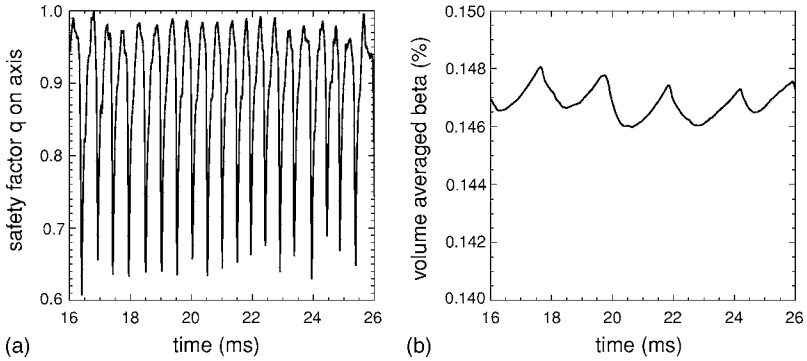


FIG. 5. (a) Central $q$ and (b) volume-averaged $\beta$. RTP-Ohmic simulation.

the experiments) also evolves from an initially monotonic one to a rather flattened time-averaged one [Fig. 2(b)]. The computed dynamo current-density [Fig. 3(a)] and zonal flow profiles [Fig. 3(b)] primarily responsible for the profile-turbulence interactions are shown. Their corrugations can be clearly seen; the dynamo currents are key to the $q=3$ sawtooth-like relaxation oscillations in the wave form of the volume-averaged $\beta$ [Fig. 4(a)] and the integrated magnetic turbulence intensity [Fig. 4(b)]. Further study shows that artificial suppression of these currents quenches the oscillations. CUTIE computes a sawtooth period of 3 ms, with amplitude $\simeq 150-200$ eV and crash time of 300 $\mu$s compared with experimental values of 1.5–2 ms, 100 eV, and 200–500 $\mu$s, respectively. The computed global energy confinement time of 3–4 ms is comparable with the experimental one of 3 ms. It should be evident that the transport thus computed cannot be obtained with a purely viscoresistive MHD code but depends crucially on two-fluid effects listed earlier.

We next present a second simulation under purely Ohmic conditions, also in RTP ($\beta \simeq 0.14\%$, $\rho_* \simeq 0.0067$, and $\nu_* \simeq 0.6$). This simulation has been done with increased poloidal resolution (64 harmonics, as opposed to 32 in the previous one, 100 radial mesh points and 16 toroidal harmonics, and time step of 25 ns, as before). The objective was to investigate if CUTIE can simulate "traditional" $m=1$, $n=1$ sawteeth oscillations associated with a $q=1$ surface. It is interesting to observe that the simulations show not only the existence of sawteeth within the $q=1$ zone [Fig. 5(a) shows the central $q$ wave form), but also "edge relaxations" apparently related to a periodically triggered ballooning instability [Fig. 5(b) shows the volume-averaged $\beta$ wave form]. The latter has a repetition time of about 2 ms, whereas the sawtooth period is about 600 $\mu$s (somewhat less than the experimental value of $\simeq 1$ ms). The dynamo current due to the $m=1$ instability plays an important role in periodic $q$-profile flattening and current/temperature exclusions from the core during the sawtooth cycle. In Fig. 6(a) we plot the temperature and density "excursions," $\Delta T_e/\bar{T}_e \equiv (T_e - \bar{T}_e)/T_e$ and $\Delta n_e/\bar{n}_e \equiv (n_e - \bar{n}_e)/\bar{n}_e$, where $\bar{T}_e$ and $\bar{n}_e$ are the respective time-averaged values at $r/a=0$, as percentages from 16 to 18 ms. This illustrates clearly the period, amplitude, and crash times (of the order of 100 $\mu$s of the central sawteeth. In Fig. 6(b) the same quantities are plotted at $r/a=0.85$ over a longer time scale (16–26 ms), showing the different character of the edge relaxation and the correlation between density and electron temperature excursions due to the relaxations. We show the computed profiles of $T_e$ and $T_i$ (time averaged) in Fig. 7(a) where we have plotted some instantaneous Thomson $T_e$ measurements. In Fig. 7(b) we plot the computed time-averaged $q$ profile and the $n_e$ profile. Some density measurements are plotted for comparison. It is interesting to note that the instantaneous experimental profile is slightly more peaked than the CUTIE calculations suggest. The Lundquist number is $S=\tau_{\rm res}/\tau_A \geqslant 10^7$ in this case. Thus the resistive layer widths are far smaller than $\rho_s$. Although the $q$ profile in the core tends to be rather flat as suggested by the Kadomtsev reconnection scenario, the detailed features of the sawteeth are related to significant two-fluid effects which affect mode rotation, snake persistence, mixing, and crash time. In Fig. 8(a) we plot the calculated dynamo current density just before the crash (18.48 ms) and 120 $\mu$s later. It is clear that the dynamo EMF tends to rapidly trans-

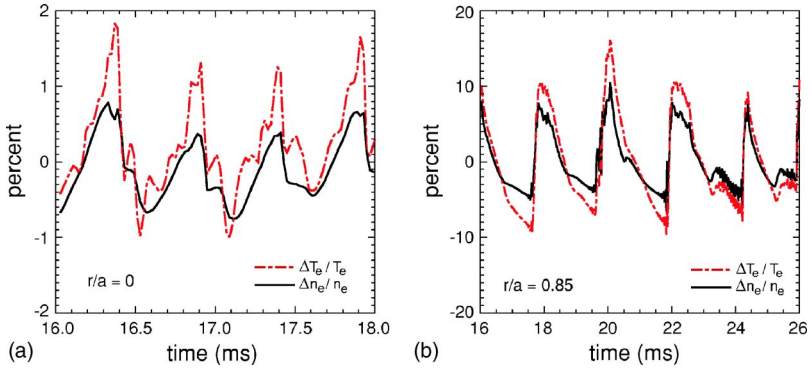


FIG. 6. $\Delta T_e/T_e$ and $\Delta n_e/n_e$ (%) (a) at $r/a=0.0$, 16–18 ms and (b) at $r/a=0.85$, 16–26 ms. RTP-Ohmic case.

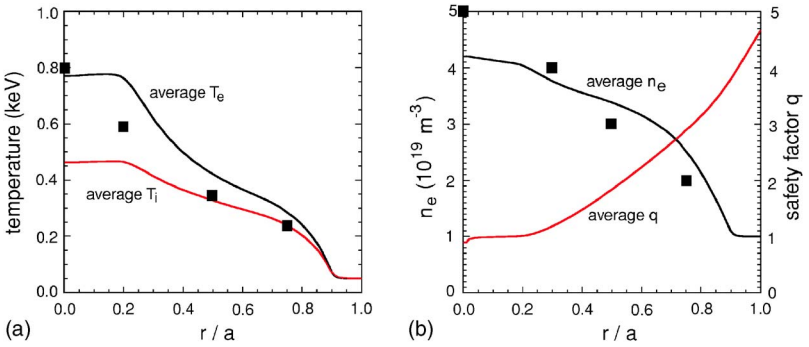


FIG. 7. Comparison of calculated (solid line), time-averaged (a) $T_e$ and (b) $n_e$ profiles with experiment (squares) in the RTP Ohmic case.

port current from the core outwards at the crash. The edge instability seems to be connected with the zonal flow gradient ($\propto E_r'$ at $r/a \simeq 0.8$; note that the plasma "edge" in CUTIE is at $r/a=0.9$; the space beyond is a simulated "vacuum" region) which stops from stabilizing the ballooning mode in question when it falls below a critical value. In Fig. 8(b) we plot the computed zonal flow profiles just before (25.1 ms) and 180 $\mu$s after the "crash." The steepening of the gradient is clearly associated with the disappearance of the mode, which also triggers edge tearing-parity drift modes $m \geqslant 4$ somewhat later (not shown, but clearly visible in movies). Figure 9(a) shows the density fluctuation contours in a poloidal plane $\delta n_e/n_e$ at a crash maximum (cf. Fig. 6(b), 21.8 ms). The ballooning character of the outermost mode ($m \simeq 10$) is evident as are the features of the inner, finer-scale ballooning modes and traces of the shear layers represented in Fig. 8(b). The mode rotation in the edge region is in the electron diamagnetic direction (anticlockwise) at this time. The contours also show the $m=1$ "snake" in the core and a "quiet" region close to $q=1$ representing an ITB. In Fig. 9(b) the same snapshot data are presented in a different way to bring out other features: we show the RMS density fluctuation Fourier amplitude $|\delta n_e/n_e|$ (summed over the toroidal mode number $n$) as a function of poloidal mode number $m$, and $r/a$ at 21.8 ms. A strongly edge-localized $m \simeq 10$ mode and a wider "mountain ridge" of fine-scale modes (with $m \simeq nq$) can be seen in the spectrogram. The $m=1$ snake in the core is also clearly visible. Thus, while dynamo currents seem crucial for the sawteeth, zonal flow shear seems to play a central role in stabilizing the edge instability. We are presently investigating the CUTIE scaling of these relaxation phenomena with the applied heating power with the aim of classifying the type of instability found.

## IV. CONCLUSIONS

We have discussed issues relating to profile-turbulence interactions and plasma relaxations using the two-fluid paradigm, as implemented in CUTIE. Although the two-fluid model is not expected to be quantitatively accurate, it does reproduce many qualitative features of electromagnetic tokamak turbulence and its influence on long-term dynamics via profile-turbulence interactions involving dynamo currents ($q$-profile effects) and zonal flow shear. Our simulations show that the turbulence as calculated by CUTIE is strong (when measured against typical "mixing length" estimates) and is mostly saturated. This clearly renders identification of particular linear instabilities which may be responsible for transport problematic, if not meaningless. A "sea" of stable and unstable turbulent fluctuations (these may be due to either to linear or nonlinear instabilities, as in neutral fluid turbulence) simultaneously coexist, perpetually exchanging energy and enstrophy in a quasistationary state, punctuated by the large-amplitude edge or core relaxations discussed. In addition, the profile gradients in density, electric field, temperatures, and current density continually fluctuate significantly about their time-averaged values, as do relevant fluxes, and turbulence-driven flows and currents. In this circumstance, one is clearly not talking about the instability of some fixed, imposed profile, as in standard linear stability analyses: at different spatial locations and times, different instabilities may arise, coexist, and modify each other by mode coupling and saturate. In broad terms, the fluid ITG modes and the collisional branches of the drift Alfvén mode are clearly involved in transport processes during periods between strong MHD which takes the form of tearing parity mode structures in the core and rotating ballooning structures

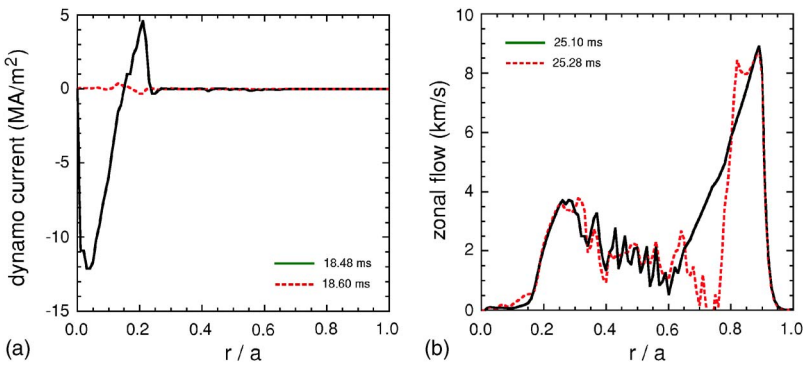


FIG. 8. (a) Dynamo currents just before and after sawtooth crash and (b) zonal flows before and after edge instability.

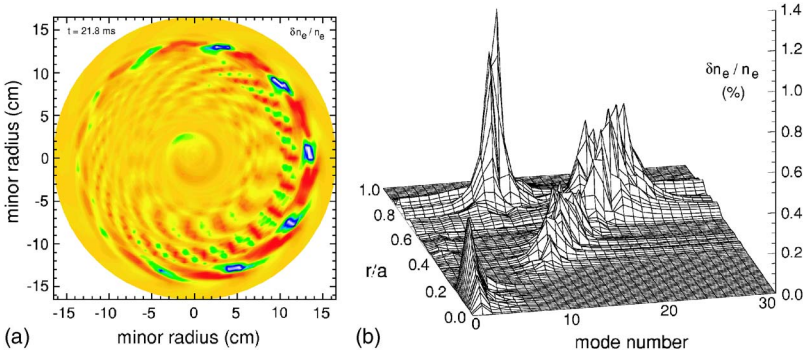


FIG. 9. (Color online). (a) Contours of density fluctuations (blue is high and red is low) and (b) $\delta n/n$ spectrogram of the same instant as in (a) (see text for definitions).

outside the heating radius. This picture is readily confirmed by movies of various fluctuation contours in a poloidal plane and by Fourier spectrograms (cf. Fig. 9). We find moreover that strong interactions between scales comparable to the system size ("macroscales") and those corresponding to the ion Larmor radius ("microscales") occur via the intermediate scales ("mesoscales"). There is no clear scale separation found in the two-fluid model. Our examples demonstrate that the turbulence can locally organize itself (and the resultant transport) through modulational instability and beat mechanisms which transfer energy to the long-wave part of the spectrum, while at the same time, the shear Alfvén waves, zonal flows, and nonlinearities efficiently transfer enstrophy via a "direct cascade" involving phase mixing to short wavelengths. This is entirely consistent with the study of simpler systems[5] which show that fast growing high-$k$ modes can easily transfer energy to the low-$k$ spectrum and enstrophy to the high-$k$ part where it will be dissipated by turbulent diffusion and phase mixing. It is therefore crucial to retain the long-wavelength modes in global simulations in order to obtain a faithful representation of the dynamics on time scales much longer than the typical turbulence decorrelation times. CUTIE and its successors will be used to investigate these phenomena in more detail in the future, using more realistic models embodying some of the effects neglected in the present simulations in the search for a deeper understanding of plasma turbulence.

## ACKNOWLEDGMENTS

We thank our colleagues Jack Connor, Jim Hastie, and Hugo de Blank for many stimulating suggestions.

This work was supported by the European Communities under the contracts of Association with EURATOM/FOM and EURATOM/UKAEA. The views and opinions expressed herein do not necessarily reflect those of the European Commission. It was jointly funded by Euratom, NWO, and the United Kingdom Engineering and Physical Sciences Research Council.

[1] A. Smedman, U. Högström, and J. C. R. Hunt, Q. J. R. Meteorol. Soc. **130**, 31 (2004).
[2] A. Hasegawa and Y. Kodama, Phys. Rev. Lett. **41**, 1470 (1978).
[3] A. I. Smolyakov, P. H. Diamond, and V. I. Shevchenko, Phys. Plasmas **7**, 1349 (2000).
[4] P. N. Guzdar, R. G. Kleva, and L. Chen, Phys. Plasmas **8**, 459 (2001).
[5] D. R. McCarthy, C. N. Lashmore-Davies, and A. Thyagaraja, Phys. Rev. Lett. **93**, 065004 (2004).
[6] A. Thyagaraja, Plasma Phys. Controlled Fusion **42**, B255 (2000).
[7] A. Thyagaraja, P. J. Knight, and N. Loureiro, Eur. J. Mech. B/Fluids **23**, 475 (2004).
[8] M. R. de Baar, A. Thyagaraja, G. M. D. Hogeweij, P. J. Knight, and E. Min, Phys. Rev. Lett. **94**, 035002 (2005).
[9] X. Garbet, C. Bourdelle, G. T. Hoang, P. Maget, S. Benkadda, P. Beyer, C. Figarella, I. Voitsekovitch, O. Agullo, and N. Bian, Phys. Plasmas **8**, 2793 (2001).
[10] R. D. Hazeltine and J. D. Meiss, *Plasma Confinement* (Addison-Wesley, New York, 1992).
[11] A. J. H. Donné, Plasma Phys. Rep. **20**, 192 (1994).
[12] M. R. de Baar, G. M. D. Hogeweij, N. J. Lopes Cardozo, A. A. Oomens, and F. C. Schüller, Phys. Rev. Lett. **78**, 4573 (1997).
[13] G. M. D. Hogeweij, N. J. Lopes Cardozo, M. R. de Baar, and A. M. R. Schilham, Nucl. Fusion **38**, 1881 (1998).